Overview of Wheel/Rail Load Environment Caused by Freight Car Suspension Dynamics

SEMIH KALAY AND ALBERT REINSCHMIDT

It has been a well-established fact that excessive wheel/rail loads cause accelerated wheel/rail wear, truck component deterioration, track damage, and increased potential for derailment. The economic and safety impact of the increased wheel rail loads can only be ascertained by a total characterization of the wheel/rail loads. In this paper, a comprehensive set of experimental results obtained from on-track testing of conventional North American freight cars using both wayside and on-board measurement systems are presented. The particular emphasis is given to the wheel/rail loads resulting from suspension dynamics. The dynamic wheel/rail environment addressed in this paper is limited to dynamic performance regimes such as rock-and-roll and pitch-and-bounce, hunting, and curving. The strong dependence of the dynamic response of a railway vehicle on a truck suspension system has been illustrated by comparison of controlled test results for vehicles of different types.

Growing understanding of the interactions between vehicle and track continues to provide benefits in both performance and safety. Recent advancements in freight car modeling and testing procedures have enhanced the understanding of wheel/rail dynamics and continue to provide guidance in dynamic system testing (*1*,*2*). Development of experimental techniques to accurately measure the wheel/rail loads using instrumented wheel sets has made it possible to determine the total load environment seen under railway cars over long stretches of track (*3*). Many large-scale on-track tests have been conducted by railway researchers to characterize the dynamic performance of railway vehicles using state-of-the-art computer-based data acquisition systems (*4*–*6*).

The Association of American Railroads (AAR) has been an active participant in conducting extensive analytical and experimental vehicle dynamics research through the years. In this paper we have attempted to bring together the results of some of the experimental research conducted by the AAR, regarding dynamic load environment for conventional freight cars.

The forces generated at the wheel/rail interface depend on many factors, such as the geometry of the wheel and rail, vehicle weight and suspension system, vehicle speed, and track stiffness and damping properties. It should not be assumed that the wheel/rail loads remain constant in magnitude and a constant increase in the static loads could accurately represent the dynamic effects. Nevertheless, most conventional techniques for vehicle and track structural design use assumed dynamic load factors that represent only the effects of maximum dynamic load conditions (*7*). The most serious problem with these types of assumptions is that they neither make any distinction for the effects of suspension design used in different types of freight cars nor describe the variety of track conditions found in revenue service. Ideally, for design of track and freight car structures, a total description of the load spectra including low-frequency high-dynamic loads should be used (*8*).

Our purpose in this paper is to provide an overall understanding of the dynamic load environment encountered under typical North American freight cars. The dynamic forces that are covered in this paper are associated with low-frequency response of the car body to lateral and vertical track excitations. The longitudinal dynamic loads that result from train action and thermal effects are excluded.

The low-frequency dynamic loads are primarily associated with vehicle suspension dynamics and cause much of the track/vehicle damage because they are transmitted to all of the vehicle and track components. The loads associated with high-frequency response, such as those from wheel/rail impacts at discrete rail anomalies and flat wheels, are not included unless they occurred in conjunction with low frequency phenomena.

We begin the paper with a brief description of the loads that take place at the wheel/rail interface and their measurement techniques. The test results obtained from a series of vertical dynamic performance tests are described: both the rock-and-roll and pitch-and-bounce responses that result from typical track irregularities are presented. On-track test results for 70-, 100-, and 125-ton freight cars using wayside and vehicle-borne instrumentation are presented. Next, measurement of vertical track irregularities using an instrumented freight car is described. The vertical load environment developed by the response of this car to both revenue and controlled test track irregularities is given. This is followed by a description of the lateral and vertical loads produced during hunting of an empty and loaded 100-ton car. Finally, the wheel and rail loads developed under steady-state and dynamic curving of 100- and 125-ton cars are presented.

DESCRIPTION OF WHEEL/RAIL LOADS

A conventional freight car consists of a load carrying body supported by two rail trucks. The standard three-piece truck uses two wheel sets connected to two side frames through a very stiff primary suspension system and a bolster connecting

Association of American Railroads, 3140 South Federal Street, Chicago, Ill. 60616.

to the side frames through a secondary suspension system. The wheels, rigidly attached to an axle, are coned to provide self-steering action for the vehicle. The primary function of the suspension system is to provide guidance and stability and to isolate the car body from random track forces.

The wheel/rail forces that take place at the wheel/rail interface are composed of three components: vertical, lateral, and longitudinal forces. The vertical forces from the static weight of the car are attenuated or accentuated in magnitude because of the dynamic effects, such as those induced by the wheel tread and/or rail surface irregularities. The lateral forces result from the response of the vehicle to lateral track irregularities, creep, and wheel flange forces that arise from lateral instability and curving. Finally, the longitudinal forces are produced by the effects of train action, traction, and braking.

In qualitative terms, the forces acting on a freight car wheel set can be viewed in two broad categories: the wheel/rail contact forces and external forces (*1*). The external forces include the suspension forces, vehicle forces from gravity and couplers, and tractive and brake forces. The wheel/rail contact forces consist of normal and tangential forces acting at the contact patch at the wheel/rail interface. The normal forces act perpendicularly to the plane of contact. For large lateral wheel set excursions, the component of the force exerted on the wheel by the rail normal to the contact patch has a large lateral component, which is referred to as the flange force. The tangential forces in the contact plane are the longitudinal creep forces acting parallel to the direction of travel and lateral creep forces parallel to the wheel set's axis of rotation. Because of the tapering, when the wheels are forced to run outside the equilibrium rolling line, wheel creep or slip takes place. Resulting elastic deformations between the wheel and rail give rise to the lateral and longitudinal creep forces that balance all the forces exerted by the vehicle suspension system. The maximum creep force occurs during gross sliding of the wheel over rail and is determined by the product of normal force and the coefficient of friction by Coulomb's law of friction.

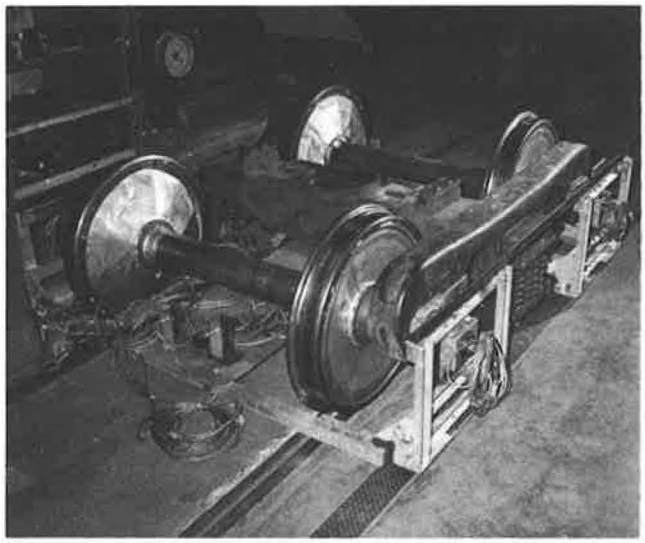

FIGURE 1 An instrumented wheel set.

WHEEL LOAD MEASUREMENTS

An accurate measurement of the dynamic forces developed at the wheel/rail contact patch is of utmost importance to characterize the dynamic performance of railway vehicles. Over the past decade, advances in finite element stress analysis techniques and electronics have made it possible to accurately measure these forces.

The instrumented wheel set and instrumented rail are the two fundamental measurement techniques for the determination of dynamic wheel/rail forces (*9–11*). In either case, strain gages are mounted on the wheel plate or on the spokes, if a spoked wheel is used, or on the rail, and the measured strains are translated into the wheel/rail forces. In either case, the triaxial components of the forces can be measured continuously.

The force measurements made by using instrumented wheel sets provide the load spectra for the specific car and the track segment it is used on. And the instrumented rail section provides the load spectra at a location in the track for a variety of cars. The wheel/rail load measuring wheel sets reported in this paper were developed by the IIT Research Institute (*11*). In this design, each wheel has strain gages mounted on the wheel plate connected to form six separate full Wheatstone bridges: three vertical, two lateral, and one position. The locations of the strain gages on the wheel plate are determined from an analytic study of strains on the surface of the wheel. The vertical bridges respond primarily to vertical loads acting on the wheel. The position bridge is used to determine the lateral position of the line-of-action of the vertical load. The remaining two bridges are used for lateral load measurements.

The electrical signals from the strain gage bridges are further processed to provide continuous vertical and lateral load measurements by using a dedicated microprocessor for each wheel set. The raw data are scaled and processed in real time to remove cross-talk effects that result from the interaction of the vertical and lateral bridge signals. Figure 1 shows such an instrumented wheel set.

VERTICAL DYNAMICS

A conventional freight car is supported by two trucks that are connected to the body through a suspension system with coil springs. As described previously, the primary objective of the suspension system is to have the wheels follow the track surface as closely as possible and to isolate the car body from the damaging vibrations induced by track irregularities. A car body supported on front and rear springs oscillates in a combination of pitching and bouncing about the center of gravity in the vertical plane. Similarly, car body roll, yaw, and sway oscillations arise from the relative motions between the vehicle and its trucks through the suspension system.

A mechanical system supported by springs will have natural frequencies that are inherent dynamic characteristics resulting from mass-stiffness effects. As a result, any mechanical system in motion will have critical speeds determined by the natural frequencies. Harmonic responses occur when the vehicle is subjected to periodic track surface irregularities such as jointed rails or even poor welds. Resonance occurs when the frequency at which the vehicle travels over the equally spaced rail joints coincides with the natural frequency of the car body on its suspension system. When resonance occurs, danger-

ously large oscillations occur, and the vehicle components experience excessive loads.

Car body roll and bounce motions are the most commonly encountered dynamic phenomena in North American railroad environment. There are two reasons for this. First, the vehicle roll and bounce natural frequencies are in the 1- to 2-H range, and resonance conditions can be induced by external forces within the operational speed range of these vehicles. Second, the track conditions that induce roll and bounce motions—staggered and nonstaggered rails—are always present in the track.

The result of excessive body roll and bounce is high dynamic loads imposed on the track and truck components resulting in spring bottoming, wheel lift, and track damage. Therefore, the effects of increased vertical and lateral wheel loads need to be investigated for their impact on maintenance and safety.

In general, response of a vehicle to staggered and nonstaggered track irregularities can be addressed by rock-and-roll and pitch-and-bounce evaluation. Both analytical and experimental methods are used in this evaluation. In the following subsections, selected results obtained from various vertical dynamics performance tests using typical 70-, 100-, and 125-ton cars are presented.

Rock-and-Roll

70-Ton Cars

In early 1986, as part of the High Productivity Integral Train Project, the Railmaster intermodal concept was tested at the Transportation Test Center in Pueblo, Colorado (*12*). The vehicle consisted of three modified highway vans with 70-ton frame-braced three-piece trucks. The trucks had a special adaptor bolster to couple the vans together. The trucks had variable column damping and D5 secondary suspension springs.

The rock-and-roll tests were run over an 800-ft tangent test section with 39-ft staggered rail joints with 0.75-in. maximum cross-level elevation. Test speeds ranged from 10 to 25 mph. The test results for the rear van are presented in the following paragraphs.

The vertical wheel loads for the leading axle of the rear truck were measured using a 33-in. instrumented wheel set. Figure 2 shows the maximum wheel loads for the right wheel versus speed, where most of the dynamic activity occurred within a critical speed range of 19 to 24 mph. At 23.3 mph, maximum wheel loads were 26 kips, and the corresponding 95th percentile of L95 values (a statistical parameter defining a level that is exceeded 5 percent of the time) was 22.7 kips. The static wheel load on this lightly loaded 70-ton truck was about 12 kips. Therefore, the ratio of a maximum vertical wheel load to its static level, representing dynamic augmentation, was about 2.2. The maximum lateral wheel loads (not shown here) were as high as 8 kips. The peak lateral/vertical (L/V) ratios resulting from the peak lateral loads were about 0.5.

The measurements of spring deflections indicated that spring bottoming did not occur during resonant roll motion of the vehicle. The maximum peak-to-peak car body roll angles were about 6 degrees.

In order to determine the load environment as affected by high curvature and cross-level variations, the same vehicle was tested in the 7.5-degree curve on the Balloon loop at the Transportation Test Center in Pueblo, Colorado (TTC). The test track had 4.5 in. of superelevation resulting in a balance speed of approximately 30 mph.

Figure 3 shows how the peak vertical loads varied as speed increased from 14 to 35 mph. Maximum wheel loads of 27 and 23 kips, experienced on the low and high rails near the critical roll speed of 23 mph, represent dynamic load factors of 2.3 and 1.9, respectively. The peak lateral loads were 9.6 kips on the low rail and 7.3 kips on the high rail at 23 mph.

The maximum vertical loads measured on the leading truck of the vehicle, which were shared by two adjacent vans, were

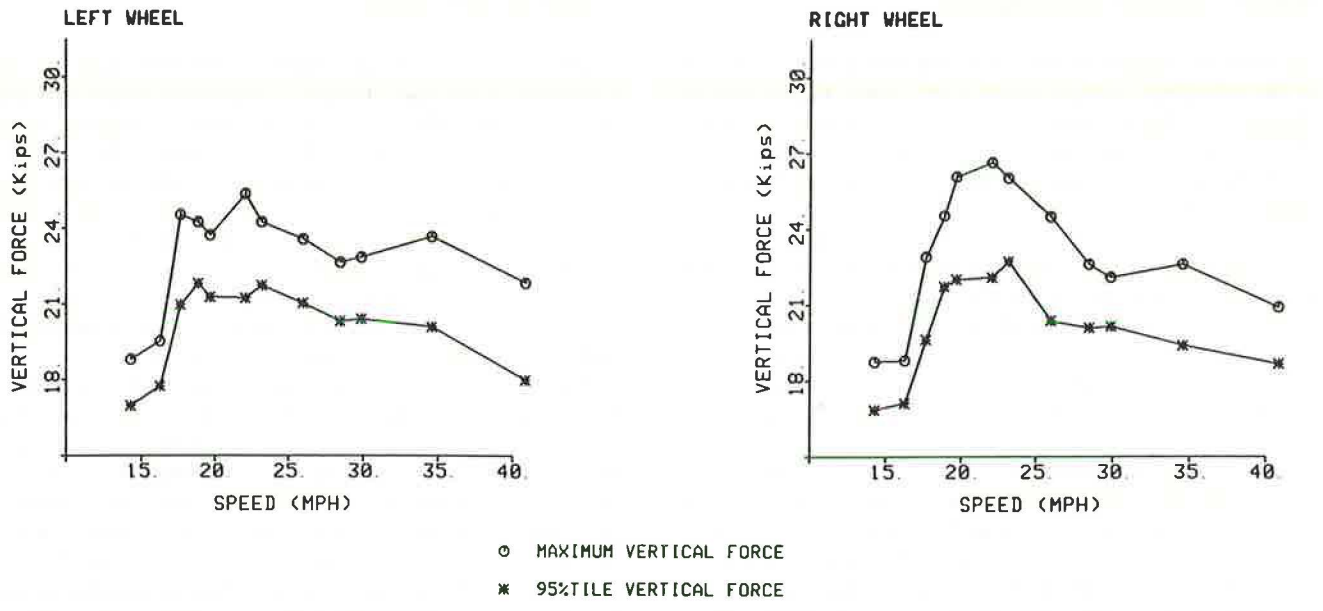

FIGURE 2 Maximum vertical wheel load versus speed for a lightly loaded 70-ton truck, measured with tangent rock-and-roll tests using instrumented wheel set data.

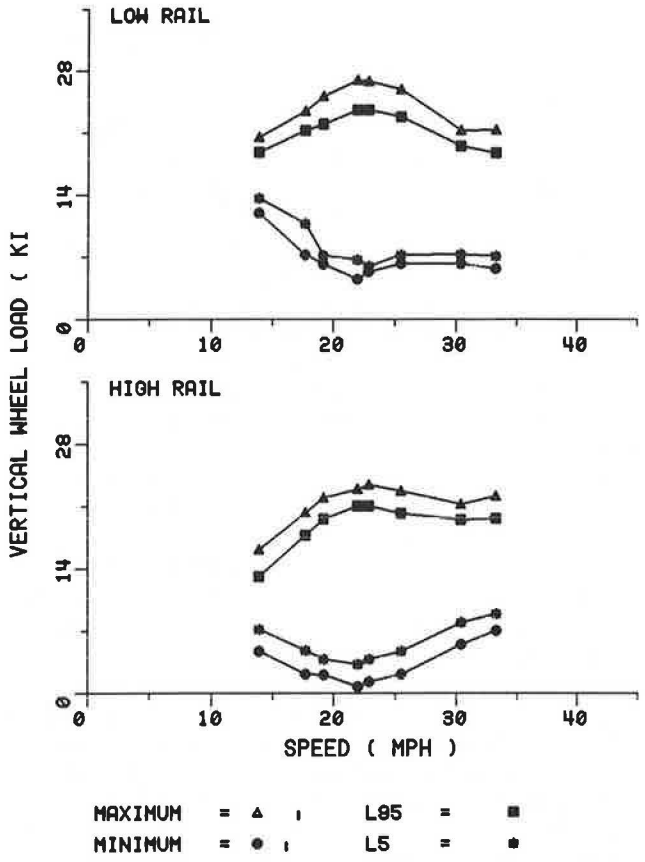

FIGURE 3 Maximum vertical wheel load versus speed for a lightly loaded 70-ton truck, measured with 7.5-degree-curve rock-and-roll tests using instrumented wheel set data.

of the same order. Peak vertical load on the high rail on the 7.5-degree curved track was about 34 kips, which represented a dynamic load factor of 1.8 (the static wheel load on the shared truck was 19 kips). The maximum lateral load on the high rail was about 12 kips. Suspension spring bottoming was not experienced at any speed at which the vehicle was tested.

In light of these results, the dynamic wheel loads produced during roll resonance of a vehicle equipped with 70-ton frame-braced trucks varied from 1.8 to 2.3. These results are not meant to represent the dynamic load environment seen under a standard 70-ton car during roll resonance. It should be kept in mind that these data are intended to provide limited information for a special freight car equipped with 70-ton trucks. We were unable to compare these results with those of the standard 70-ton cars because the experimental studies leading to quantification of the dynamic load environment under standard 70-ton cars are not well reported in current literature.

100-Ton Cars

As part of the High Performance Covered Hopper Car Project (*13*), one of the most comprehensive on-track dynamic performance test series of 100-ton covered hopper cars was conducted at the TTC in the early 1980s. The vehicle was instrumented with transducers to measure the accelerations and displacements at both the car body and truck levels. Instrumented wheel sets were used on the leading truck of the test vehicle to measure the vertical and lateral loads during rock-and-roll motion of the vehicle. The tests were run over 400-ft tangent and 7.5-degree curved test sections, with 39-ft staggered rail joints set at 0.75-in. cross-level elevation. Test speeds ranged from 10 to 25 mph.

Figure 4 shows the maximum and minimum levels of the wheel loads for the loaded car on tangent track. Peak maximum loads were developed at speeds near resonant roll speed of the vehicle. The maximum wheel load experienced at the critical roll speed of 17 mph—78,000 lb—represents a dynamic load factor of 2.4. It is seen from this figure that in a speed range from 15.5 to 18 mph, extended wheel lifts occurred. During maximum roll response, the car body rolled as much as 10 degrees peak-to-peak.

The dynamic loading and unloading of the leading axle of the leading truck were also very severe on the curved track. Figures 5 and 6 show peak low- and high-rail vertical loads with respect to vehicle speed. Near the critical roll speed of

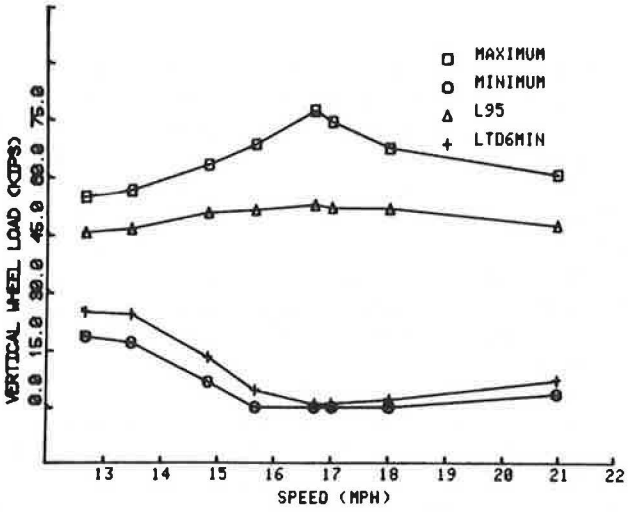

FIGURE 4 Vertical wheel loads under a 100-ton loaded hopper car, measured with tangent rock-and-roll tests using instrumented wheel set data.

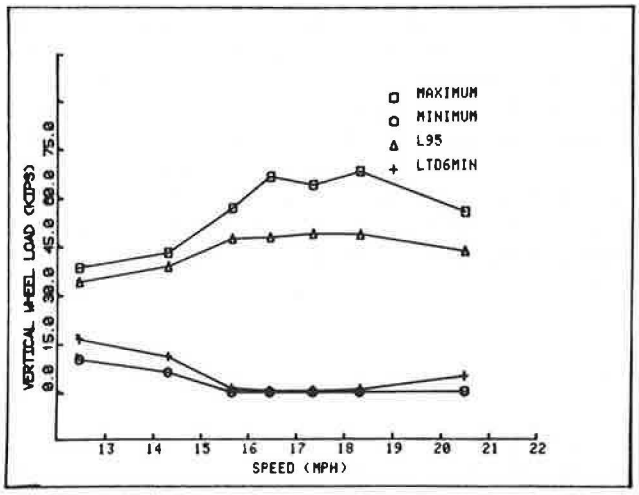

FIGURE 5 High-rail vertical wheel loads for a 100-ton loaded hopper car, measured with curved track roll tests.

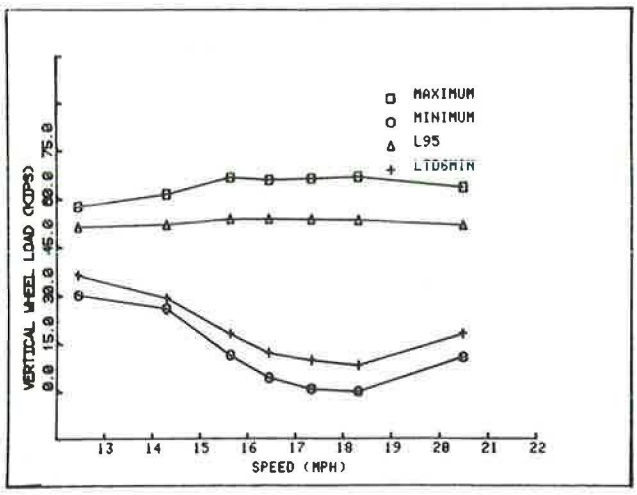

FIGURE 6 Low-rail vertical wheel loads for a 100-ton loaded hopper car, measured with curved track roll tests.

17 mph, the peak loads were as high as 68,500 lb on the high rail. At speeds ranging from 15.5 to 18.5 mph, extended wheel lifts occurred on the high rail; duration of 100 percent wheel unloading was at least 250 sec. The low-rail loads were higher than the high-rail loads, consequently the low-rail wheel unloading was less than that of the high rail. It should be noted that, on a 7.5-degree curve with 4.5-in. superelevation, higher dynamic loads develop on the low-rail side because of the offset of the car's center of gravity resulting from unbalanced running conditions, along with the increased roll in the low-rail direction.

In conclusion, the peak vertical loads developed during resonant roll motion of the 100-ton loaded car on tangent and curved tracks were comparable and equally severe. In both cases the measured loads were more than twice the static wheel load, and the resulting car body roll angles were as high as 10 degrees peak-to-peak.

Track loading resulting from rock-and-roll motions of a vehicle at critical speeds is severe. As a result of excessive body roll, the weight of the vehicle may shift into the side bearings. Suspension spring bottoming occurs, and resulting violent undamped motions cause excessive loading of one side of the vehicle with the other side lifting clear of the track. The asymmetric loading of the track structure along the direction of travel produces excessive stresses on the track components at the weakest point in the track structure resulting in accelerated deterioration and additional loss of track geometry. With increasing cross-level elevation, the vehicles operating over the same track section experience higher and higher loads bringing about additional geometry loss resulting in increased derailment propensity.

125-Ton Cars

The 125-ton dynamic load environment is relatively new to the railroads, but it is getting increased attention in recent years, particularly with the upcoming Facility for Accelerated Service Testing (FAST) tests. Preliminary tests consisted of a series of rock-and-roll tests using a consist of five 125-ton covered hopper cars. These tests were conducted at the TTC in early 1988 to quantify the loading environment and response of a typical track under heavy axle loads.

The test track consisted of 20 39-ft staggered rail sections with a maximum of 0.75-in. cross-level difference. Three adjacent cribs were instrumented for vertical and lateral load measurements. As shown in Figure 7, at speeds from 16 to 20 mph, coincident with the critical roll speeds of the vehicles, dynamic rail loads ranging from 80,000 to 110,000 lb, accompanied by excessive wheel unloadings, were measured.

Figure 8 shows the maximums of all of the wheel loads measured under the fourth car, which had the worst response characteristics. The vehicle appears to experience its maximum amplitude response near 16 mph, with the exception of the leading axle of the leading truck, which had increasing loads.

Vertical loads presented for the 125-ton cars were measured using wayside instrumentation. Instrumented wheel set data, which represent a continuous wheel load trace over all 20 irregularity waves, are not currently available for this car.

However, wheel load data taken from an instrumented wheel set of a 125-ton truck equipped with a primary suspension system are available (*14*).

This vehicle was tested on the same perturbed roll track at TTC over a speed range of 10 to 25 mph. At the resonant roll speed of 18 mph, probability distributions of the left vertical and lateral wheel loads over both the tangent and rock-and-roll sections are presented in Figures 9 and 10, respectively. The tangent track response was obtained at the same speed on the track section located just before the perturbed track. The distribution curves were plotted on Gaussian probability paper, so that the characteristics of the probability distribution functions are emphasized. The solid straight line in these plots is typical of random data, and it represents the measured distribution function of the instantaneous values of the wheel loads on the smooth tangent track. In the case of the roll response, the typical distribution functions give nonlinear plots, typical of sinusoidal waveforms. The low probability events represented by the tail ends of the distribution curve correspond to excessive wheel loading and unloading.

For this vehicle, the maximum vertical and lateral wheel loads were 77,000, and 33,000 lb, respectively. It is seen from the results for the two 125-ton trucks, one equipped with a primary suspension system and one without, that the dynamic loads seen under premium trucks were 40 percent lower. In other words, the maximum dynamic load factor for the standard truck was 2.8 times the static load, as compared with the premium truck, which had a maximum wheel load of 1.8 times the static load.

Pitch-and-Bounce

70-Ton Cars

Fatigue analysis of freight cars adapted by the AAR recommends the collection of load spectra for different types of cars over a broad range of track at a variety of train speeds. While collecting environmental load data from the operation of a 70-ton boxcar during FEESTs (freight equipment environmental sampling tests), bolster loads in excess of 1.8 *g* were

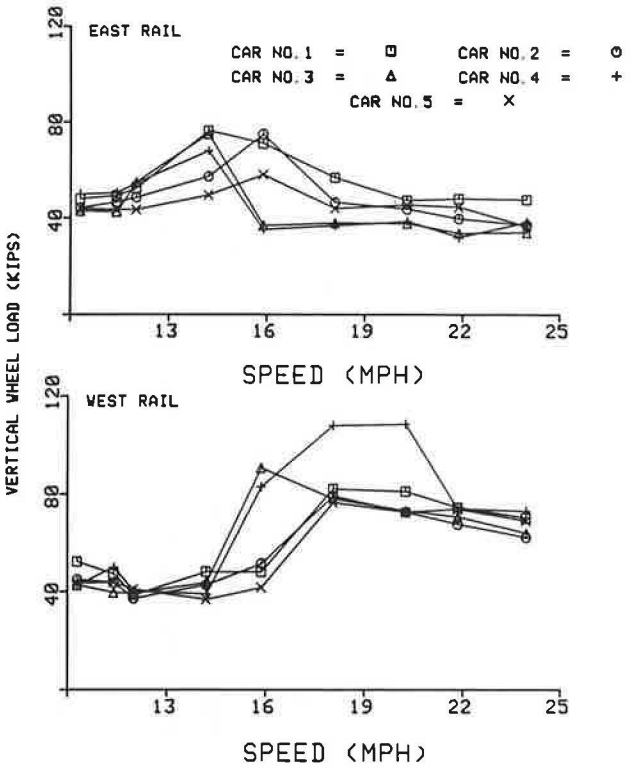

FIGURE 7 Vertical rail loads under a 125-ton loaded covered hopper car, measured with tangent track bounce tests using wayside data.

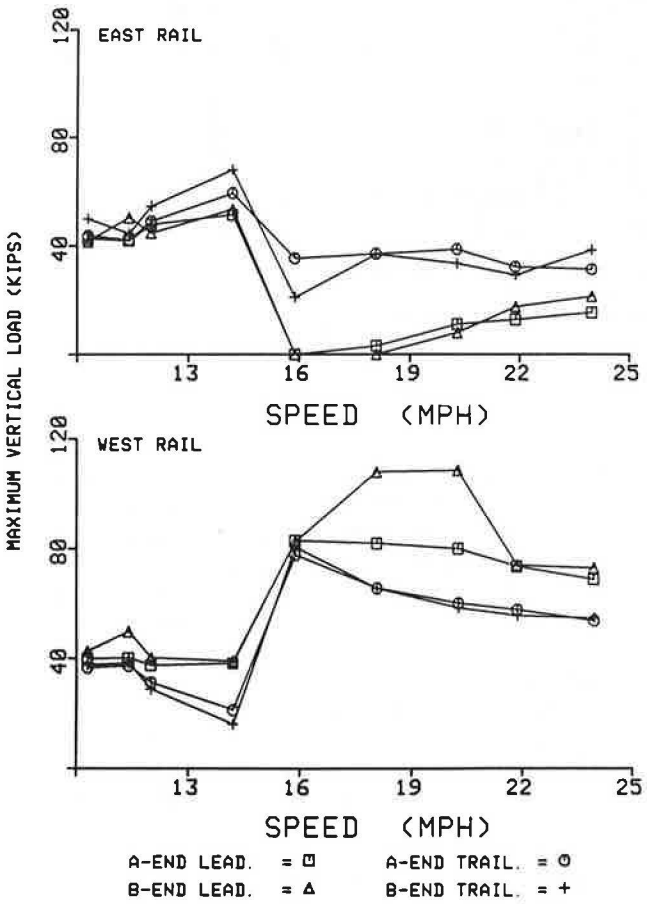

FIGURE 8 Vertical rail loads versus speed for a 125-ton loaded hopper car, measured with tangent rock-and-roll tests using wayside data.

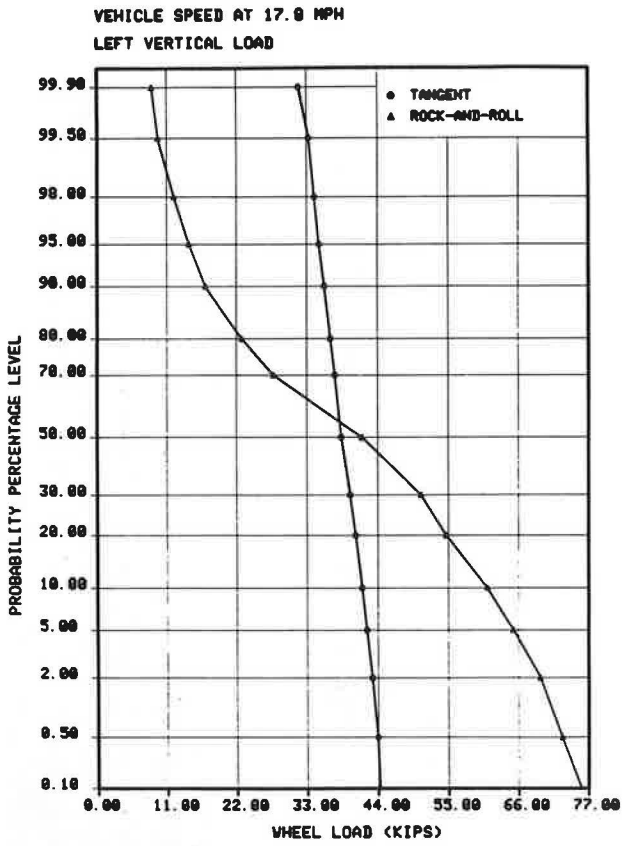

FIGURE 9 Probability of distribution of vertical wheel loads for a loaded 125-ton truck, measured using instrumented wheel set data.

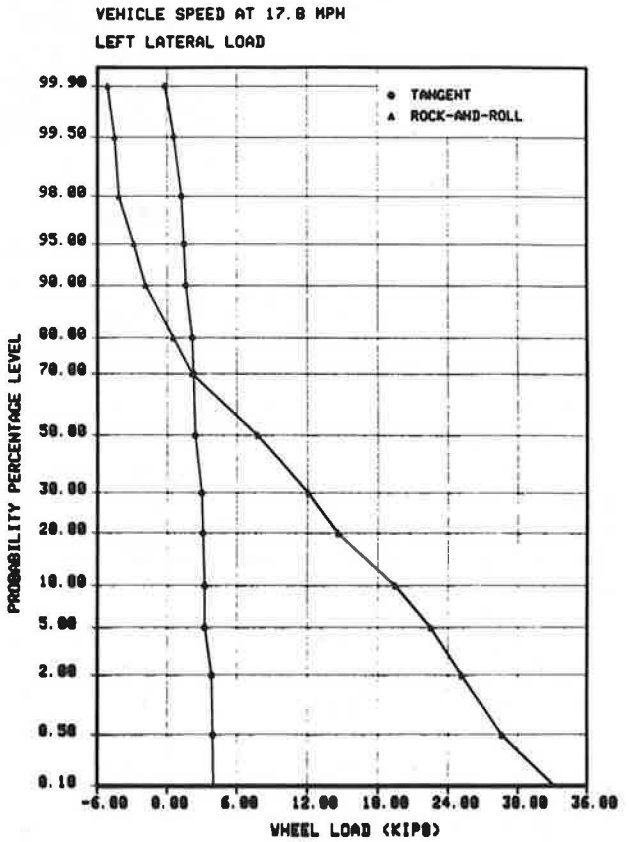

FIGURE 10 Probability of distribution of lateral wheel loads for a loaded 125-ton truck, measured using instrumental wheel set data.

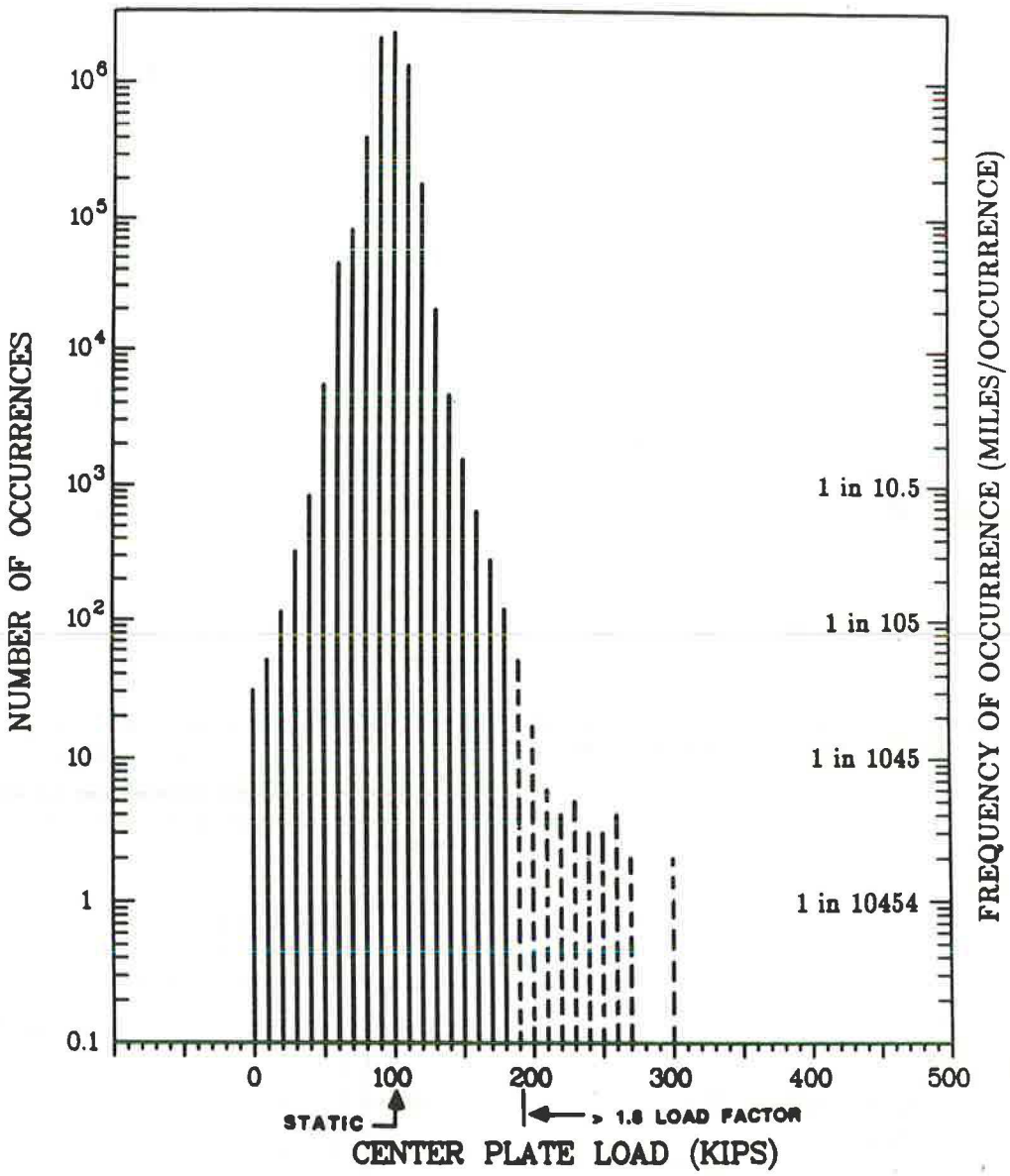

FIGURE 11 Histogram of center plate loads for a 70-ton loaded boxcar, measured with FEESTs using instrumented truck bolster data.

experienced (*8*). An analysis of the effects of the loads that are in excess of the design values on the fatigue life of a freight car was made. It was found that these high-magnitude, low-occurrence loads cause considerable fatigue damage. Figure 11 shows the occurrence histogram of center plate loads, collected over 12,000 mi for a fully loaded 70-ton boxcar. It can be seen from this figure that the design value of 1.8 *g* is exceeded, approximately two times every 100 mi.

In order to locate the track geometry that causes these high loads, the 70-ton boxcar was instrumented with a new unattended data collection system and operated in conjunction with a track geometry car on a major railroad (*15*). A paint-spray system was installed on the test car to identify the location of these high loads.

Sixteen locations were identified and spotted with a deposit of yellow paint on the track at each location. The measured loads varied from 183 to 328 kips on the bolster, which had a static load of 100 kips. The track irregularity sites that caused these high loads fell into two broad categories: those that were characterized by a single irregularity and those that had multiple irregularities.

The single irregularities were usually associated with some type of weak track segment, such as an insulated rail joint, field weld, or engine burn, causing the car to exhibit a pitch response.

Inspection of the multiple irregularity sites indicated that the load-producing irregularities were associated with open track on continuously welded rail having a series of parallel vertical irregularities at intervals equivalent to the rail length of 39 ft. At all sites examined, the dips on the track were coincident with the plant welds on one rail. Figure 12 shows the bolster load time history at a multiple irregularity site where a maximum load of 328 kips was measured.

The paint-spotter tests, in effect, showed that a series of

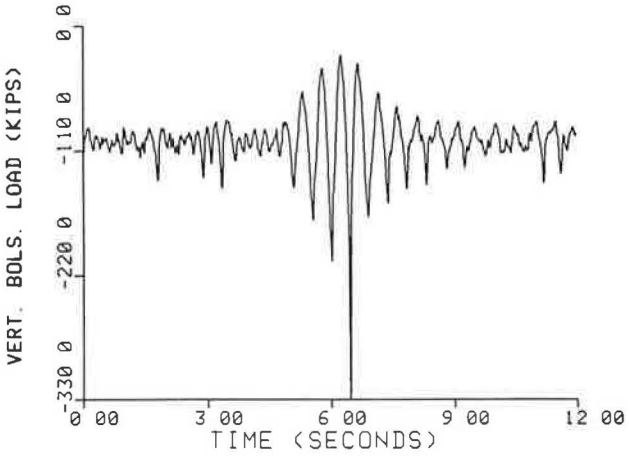

FIGURE 12 Truck bolster load time history for a 70-ton boxcar at 63 mph at a multiple irregularity site.

track profile irregularities can cause car loads in excess of the design level.

The same 70-ton boxcar was further tested under controlled conditions at the TTC's bounce section, which had 10 39-ft nonstaggered vertical irregularities with a maximum amplitude deviation of 0.75 in. (*16*). Both vehicle-borne and wayside instrumentation were used. Truck bolster loads and vertical rail loads were measured at speeds from 30 to 75 mph. The track was instrumented for vertical rail load measurements at the seventh irregularity wave.

The results of the tests showed that truck bolster vertical loads as high as 550,000 lb and car body accelerations as high as 5 *g*, accompanied by consecutive cycles of suspension bottoming and center-plate lift-off, were experienced at a critical bounce speed of 65 mph. Figure 13 shows the maximum and minimum bolster loads plotted versus speed. The vehicle responds to track irregularities with lower vibration amplitudes at speeds from 30 to 50 mph. In this speed range, the bolster loads fluctuate slightly above and below the static load of 100,000 lb, because the suspension system effectively isolates the car body from the external disturbances provided by track irregularities. At speeds near 65 mph, the dynamic activity at both the truck and car body levels sharply increases, indicating a resonance condition. At this speed, the vehicle experiences its maximum bolster load of 550,000 lb and a minimum bolster load of zero.

The results of the track testing using wayside instrumentation are shown in Figure 14, where the maximum wheel/rail loads measured on the seventh irregularity wave are plotted with respect to test speed. A typical bounce resonance characteristic is seen from this figure. The wheel/rail loads sharply increase at speeds above 60 mph, peak at 65 mph as a result of bounce resonance, and decrease as speed increases with the track-forcing-frequency becoming outside of the range of the car body's natural bounce frequency. The truck loads shown in Figures 13 and 14 are not directly comparable because the peak loads shown in Figure 13 occurred on the eighth irregularity wave. However, the maximum load exerted on the test track (the seventh irregularity wave) by the leading truck approaches 420,000 lb—extremely high for any track structure to withstand without experiencing some level of permanent damage.

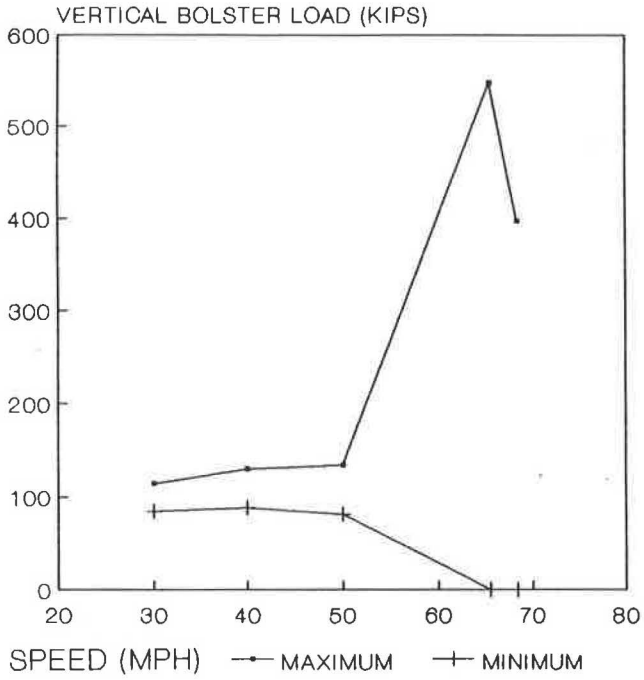

FIGURE 13 Maximum and minimum bolster loads versus speed for a 70-ton boxcar, measured with vehicle bounce tests.

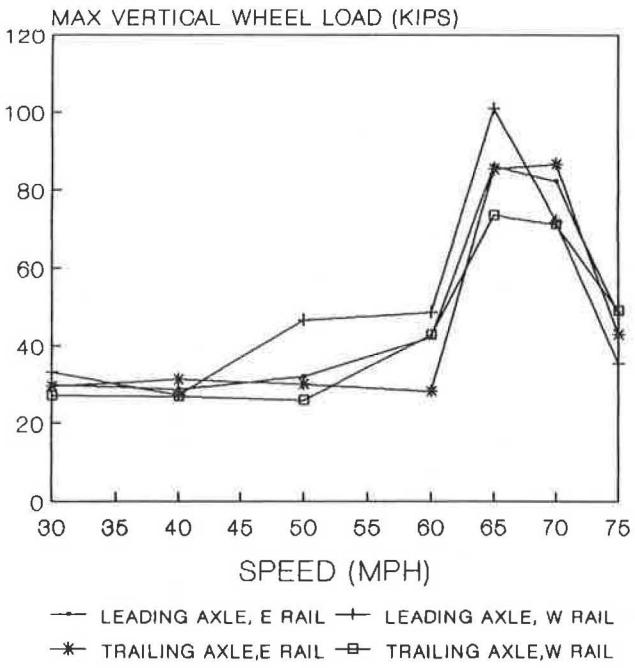

FIGURE 14 Maximum vertical rail loads versus speed for a 70-ton boxcar, measured by bounce tests using wayside data.

100-Ton Car

A 100-ton coal car was tested together with the above 70-ton boxcar for bounce characterization. Figure 15 shows the measured wheel/rail loads at each instrumented crib location at 67 mph, near resonance bounce speed. The leading truck loads peak at the sixth instrumented crib, near the peak of

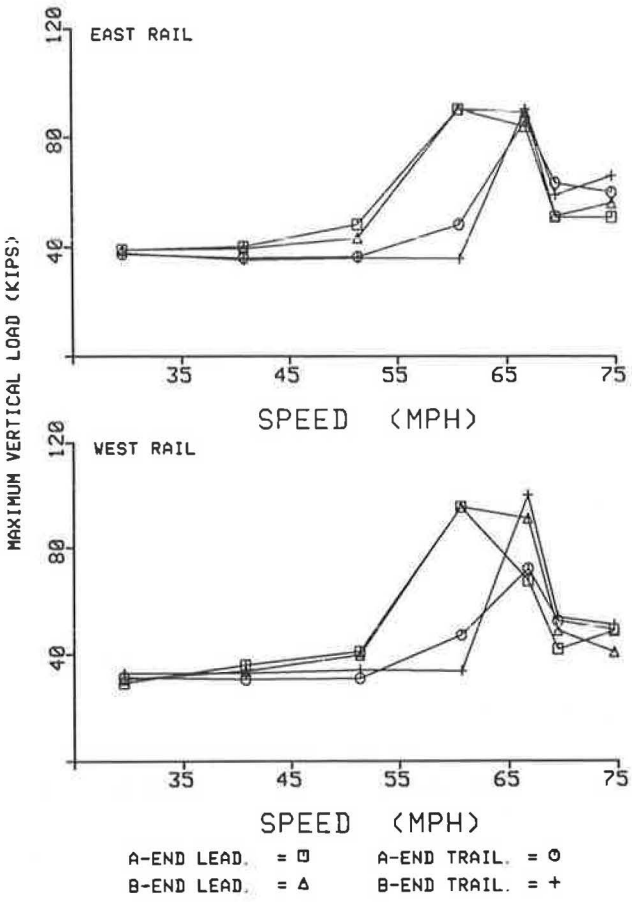

FIGURE 15 Vertical rail loads versus speed for a 100-ton loaded coal car, measured with bounce tests using wayside data.

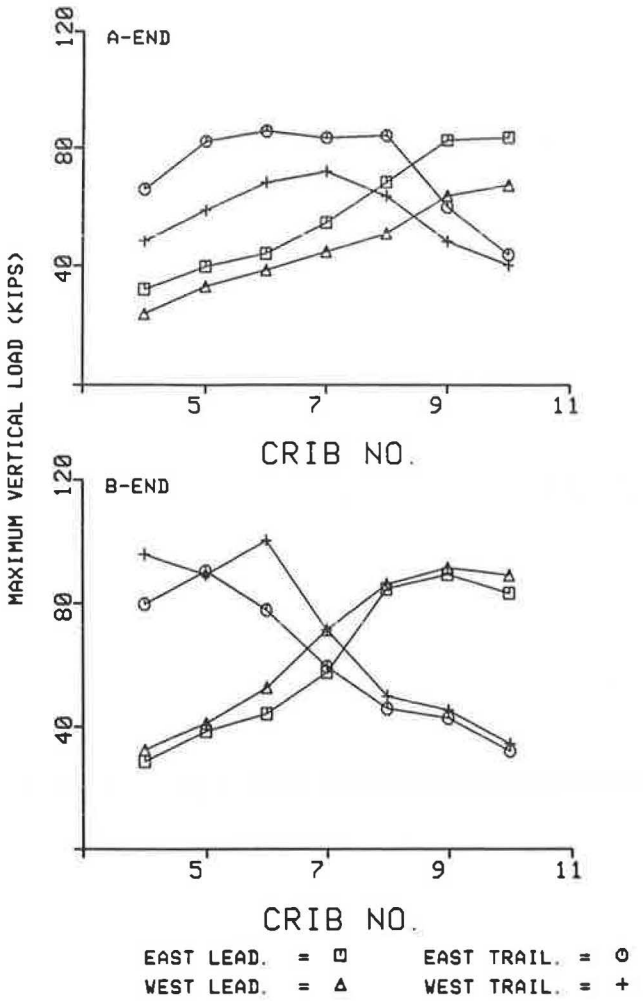

FIGURE 16 Vertical rail load at each instrumented crib for a 100-ton hopper car, measured at 65 mph with bounce tests.

the track irregularity wave. Note that the distance delay between the load peaks of the leading and trailing trucks results from a 70-in. 100-ton truck wheel base (distance extending over four instrumented cribs).

Figure 16 shows a plot of vertical wheel loads as a function of test speed. At speeds between 60 and 65 mph, the vehicle exhibited a severe bounce resonance condition in which the oscillation amplitudes were limited only by the available friction in the suspension system if the springs did not bottom out. The measured wheel/rail loads reached levels above 100,000 lb on a car with 33,000 lb of static wheel load. Above the resonant speed, the vehicle traveled smoothly over the track irregularities with considerably attenuated response amplitudes as the track irregularities were taken up by the suspension springs.

The total vertical bolster load environment encountered by standard 100-ton open hopper and hi-side gondola cars was also measured during FEESTs. Figure 17 shows the frequency of occurrence diagram for the 100-ton loaded open hopper car center plate loads collected over several thousand mi of revenue track at a wide range of operating speeds. Note that the static load on the bolster was about 120 kips. As shown in Figure 11 for the 70-ton car, a considerable number of occurrences is seen at levels above 1.8 times the static load. Also note that the maximum test speed was 60 mph, and the average test speed was 23.3 mph. Similar load levels were reported for the hi-side gondola car in unit train service (AAR-M1001).

125-Ton Cars

A train consist having five 125-ton covered hopper cars—the same consist for which rock-and-roll performance was described earlier—was tested over the same perturbed track for bounce performance. Eleven consecutive cribs were instrumented for vertical rail load measurements.

Figure 18 shows the variation of vertical wheel loads of one of the 125-ton cars over the instrumented track section at 69 mph. The dynamic signal clearly represents the dynamic load response resulting from the track irregularity. The maximum rail load measured on the east rail under the trailing truck was as high as 150,000 lb, which represents a dynamic load factor of 3.9. Evidently, the rail loads under the leading axles on each truck peak first toward the middle of the instrumented track, and the trailing axle loads increase to peak toward the end of the instrumented track because of the time delay introduced by the wheel base. Both the leading and trailing trucks exhibit similar response characteristics partly because of the truck center distance of 36.5 ft, which is fairly close to the irregularity wavelength of 39 ft.

For the five cars tested together, the measured rail loads ranged from 60,000 to 150,000 lb at the maximum test speed of 70 mph, depending on the car types, as shown in the vertical

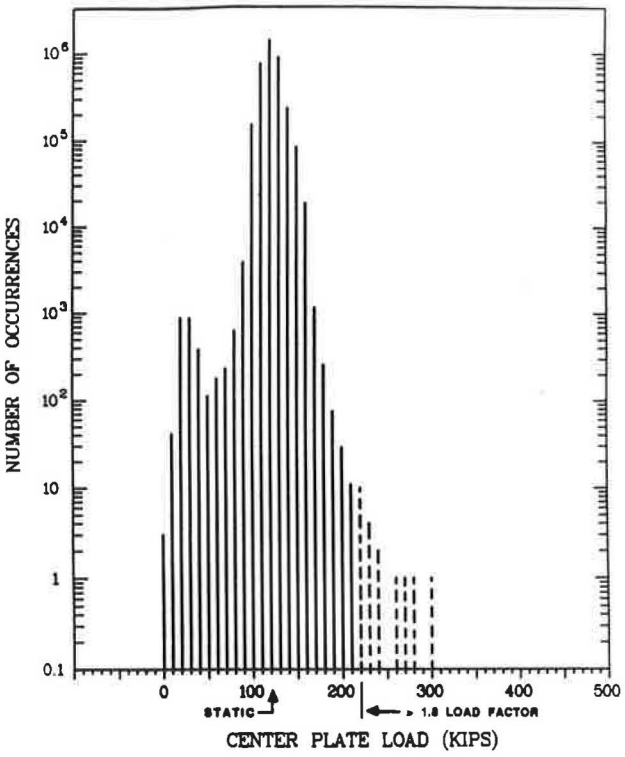

FIGURE 17 Histogram of center plate loads for a 100-ton loaded open-top hopper car FEEST test using instrumental bolster data.

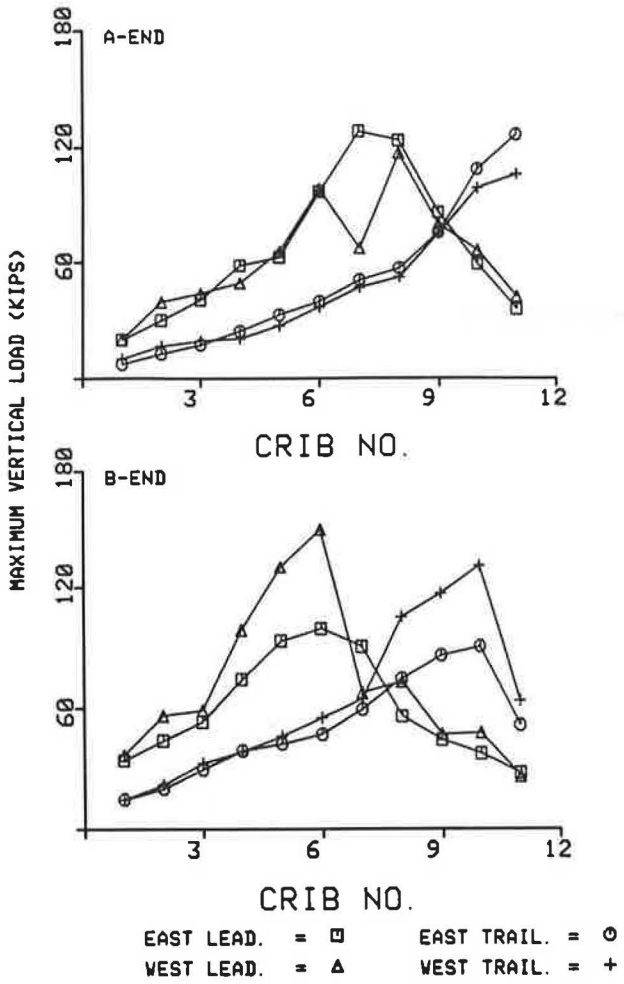

FIGURE 18 Variation of vertical rail loads over instrumented track for a 125-ton loaded car.

load versus speed plot in Figure 19. As seen from this figure, the high-peak loads consistently occurred under two of the 125-ton cars. The maintenance history of these cars is unknown, and it is likely that some suspension characteristic, related either to truck type or physical condition of the trucks, is the primary cause of these high loads. Several follow-up activities are currently under way to help understand the origin of these loads and develop possible corrective actions that might limit the peaks.

The third 125-ton car, the bounce performance of which was given in Figure 19, was tested at a later date by using instrumented wheel sets at the leading axle of the leading truck. Figure 20 shows the variation of the vertical wheel load as a function of speed. The peak load at 70 mph was as high as 130 kips, as shown in Figure 19. Figure 20 shows a comparison of wayside loads to instrumented wheel set loads, with an excellent agreement achieved at almost all test speeds. Truck suspension dependency of a vehicle's bounce response is clearly illustrated in Figure 21, in which the track loads measured under a train consist include, in order, a six-axle locomotive, FRA's T-7 instrumentation car, two 100-ton covered hopper cars, and the aforementioned 70-ton boxcar.

The locomotive and the instrumentation car, which are equipped with premium trucks with both primary and secondary suspension systems, exhibit superb bounce responses. For these cars, no apparent resonant condition is observed, and the dynamic loads virtually remain slightly above the static wheel loads. Obviously, the worst among them all is the 125-ton car tested over the same track at the same speeds.

The data presented here indicated that the vertical loads developed during bounce resonance can be extremely high. The peak dynamic loads measured under the 70-, 100-, and 125-ton cars during bounce resonance varied from 2 to 5 times the static wheel loads. Considering that the track is loaded to a maximum level under a bouncing truck, the transmission of the total load to all track components would lead to serious problems, such as (a) vertical geometry loss resulting from permanent settlement, (b) component fatigue, (c) ballast breakdown, and perhaps (d) subgrade failure.

It should be noted that the data presented here pertain to standard vehicles with average physical condition. The strong dependence of the dynamic bounce response of these vehicles on the suspension system was clearly seen from the data. The 125-ton covered hopper car data are intended to be used for comparison purposes only, because they do not represent the future 125-ton fleet, which may have premium suspension systems.

HUNTING

In some mechanical systems, self-induced oscillations can be maintained by energy sources having no oscillatory properties. The energy sustaining this motion is created by the vibration itself. In railway vehicles, the self-excited lateral oscillations, referred to as hunting, begin spontaneously at a threshold speed. This lateral instability is promoted by the

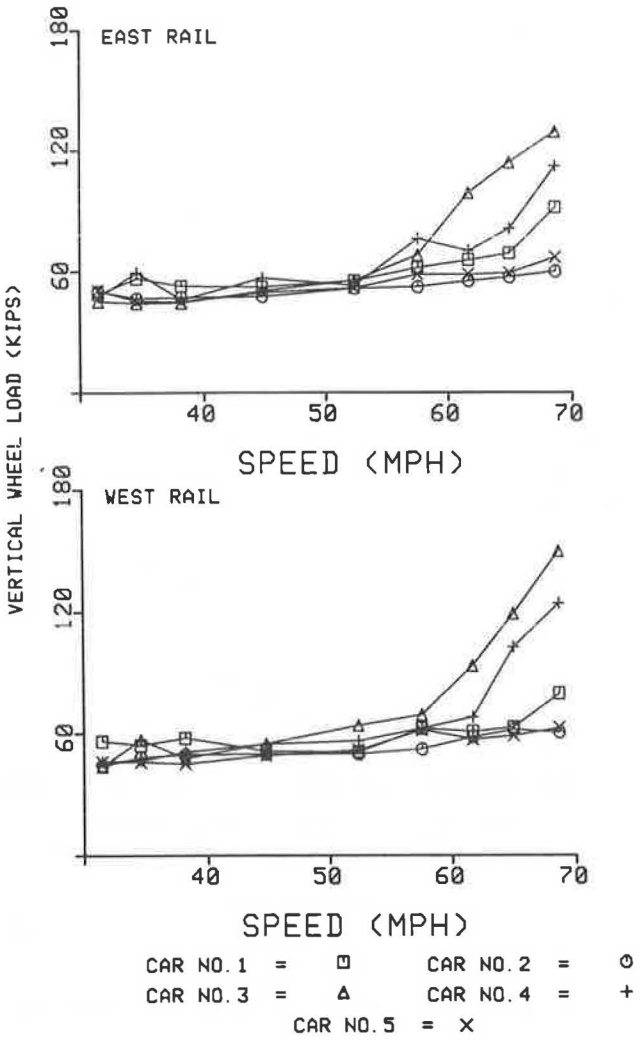

FIGURE 19 Vertical rail loads versus speed for a 125-ton loaded hopper car, measured with bounce tests using wayside data.

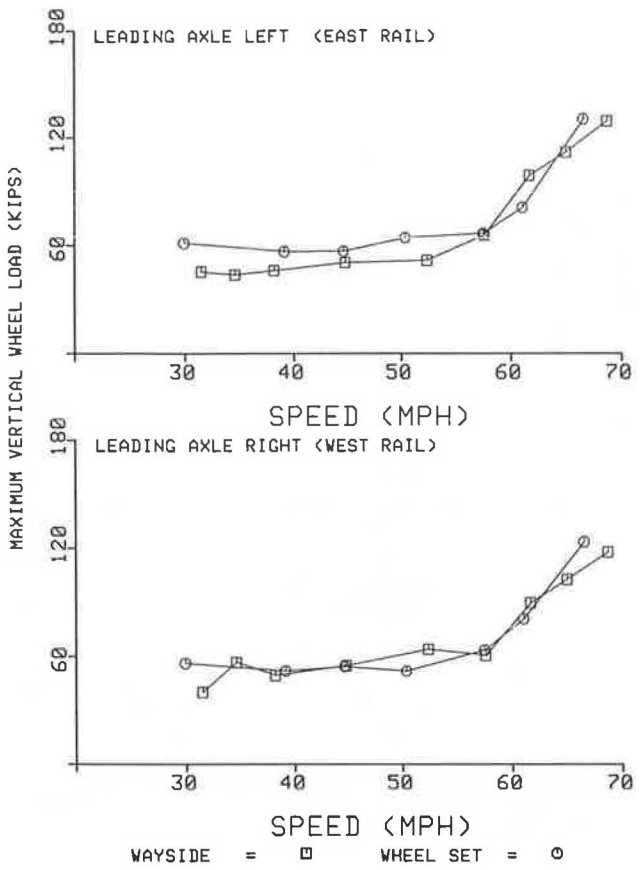

FIGURE 20 Maximum wheel load comparison of wayside and instrumented wheel set measurements from bounce tests of a 125-ton covered hopper car.

self-steering behavior of the coned wheels, and the energy to sustain this motion is provided by the wheel/rail force feedback system.

When the lateral equilibrium state of the vehicle becomes unstable, any initial perturbation (such as that from changes in the rail head profiles, as well as irregularities in the lateral alignment and rail gage) causes the amplitudes of the oscillations to increase. With increasing vehicle speed, one of the truck vibrational modes becomes the least damped mode, and larger oscillations can develop. If the oscillations are large enough, any further increase in the amplitude is precluded by the wheel flanges. In this steady-state-like limit-cycle motion, the amplitude and frequency remain constant.

70-Ton Cars

The Railmaster intermodal concept (its dynamic load environment resulting from rock-and-roll was described previously) was tested for high-speed lateral stability on tangent track at TTC (*12*). The test consist included a locomotive and the three-van Railmaster intermodal car. The trailers were empty, and the trucks were equipped with 70-ton cross-braced trucks with Canadian National Heumann profiled wheels. The test runs started at 30 mph, and a speed increment of 5 mph was chosen. The test runs continued until it was determined that the onset and sustained hunting conditions had been observed or the 80-mph speed limit had been achieved.

The measurements used for the hunting tests included lateral accelerations and displacements at car body and truck levels. The lateral and vertical wheel loads were measured on the leading axle of the lightly loaded rear truck of the rear van using an instrumented wheel set. The analyses of lateral accelerations indicated that the first sign of hunting manifested itself in increased lateral activity at 60 mph. At 70 mph, fully sustained hunting motion was observed at both the truck and body levels of the rear van. At 65 mph, the rms lateral acceleration on the rear truck was about 0.2 *g*. It should be noted that the vehicle was equipped with cross-braced trucks, which provide better lateral stability than the conventional three-piece trucks because of increased interaxle shear stiffness.

The lateral loads at the leading axle of the rear truck were investigated to determine the effects of hunting motions at the wheel/rail interface. The peak lateral loads are shown in Figure 22 as a function of speed. The maximum lateral loads increase with speed to about 5 kips on both wheels at 70 mph, but the 95th percentile of the lateral loads was a maximum of 2.5 kips. It was concluded from the results of the lateral

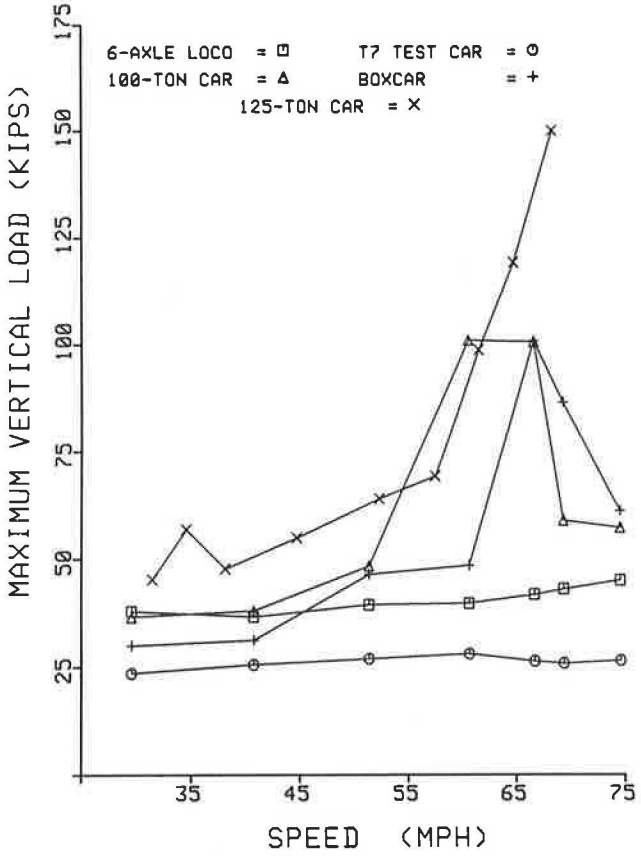

FIGURE 21 Vertical load environment under typical railroad cars, measured with bounce tests.

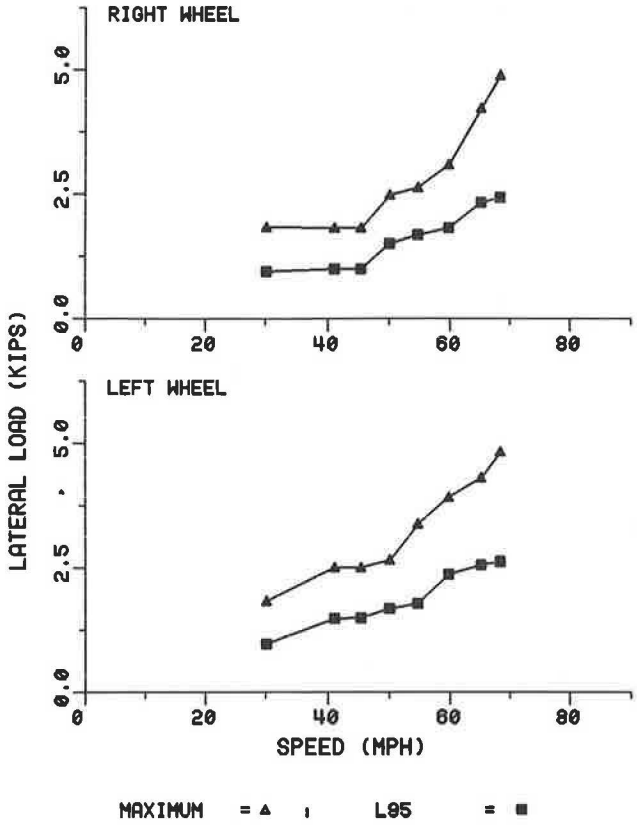

FIGURE 22 Peak lateral wheel load versus speed for a 70-ton truck, measured using instrumented wheel set data.

load response that, during hunting motion of the rear truck, sustained wheel flanging was not evidenced.

100-Ton Cars

As part of the High Performance, High Cube, Covered Hopper Car Project (*4,17*), a 100-ton covered hopper car of current design was tested for dynamic performance at the TTC. The vehicle was instrumented with transducers to measure the accelerations and displacements at both the car body and truck levels. Instrumented wheel sets were used on the leading truck of the test vehicle to measure the vertical and lateral loads of a hunting vehicle. The tests were run on a mile-long tangent track at speeds from 30 to 70 mph, in 5-mph increments. The dynamic load environment developed under the test car is presented in the following paragraphs.

The lateral loads produced at the onset of hunting, as well as those developed during fully sustained hunting, are shown in Figure 23. Absolute peak and L95 lateral load levels on the leading axle show a sharp increase at 51 mph, indicating the onset of hunting. Peak lateral loads of up to 15,300 lb were developed at speeds above 60 mph when the wheel flanges hit against the rails during violent hunting motions of both the car body and its trucks. The frequency of this motion took place at about 3.5 H, as seen in the time history plot of Figure 24.

Truck hunting is not a prevalent loaded car phenomenon because of the stabilizing effect of the increased axle load on hunting. It does, however, occur at relatively higher speeds than on an empty car. The loaded car hunting tests were conducted by using the same test car on the same tangent track on which the empty car was tested. The lateral wheel/rail forces recorded at the wheel/rail interface are shown in Figure 25, in which the sharp increase in the load levels at 60 mph indicate the onset of hunting. Peak maximum and L95 lateral loads experienced on the left wheel of the leading wheel set were about 18,000 and 13,500 lb at 71 mph, respectively. The lateral loads shown in Figure 26 imply that, during sustained hunting, frequent flange contacts occurred.

At and above the critical hunting speed of a vehicle, the wheel flanges contact the rail resulting in excessive wear of the wheels and rails and increased maintenance. During hunting, large lateral loads are exerted on the vehicle and track. These loads tend to develop wide gage (*18*) and lateral alignment problems on track. Truck hunting, when combined with track irregularities, creates a potential for derailment. Moreover, the excessive lateral and yaw motions of the wheel set increase the rolling resistance, resulting in increased energy consumption.

Despite being conducted on well-maintained, good quality track, both the empty and loaded car hunting tests indicated severe high-frequency lateral wheel loads, which changed direction as the wheel sets moved from flange to flange. These loads were certainly capable of creating high alternating stresses. These stresses could cause fatigue damage of the wheels and various vehicle components, as well as the rails, while weakening the track structure.

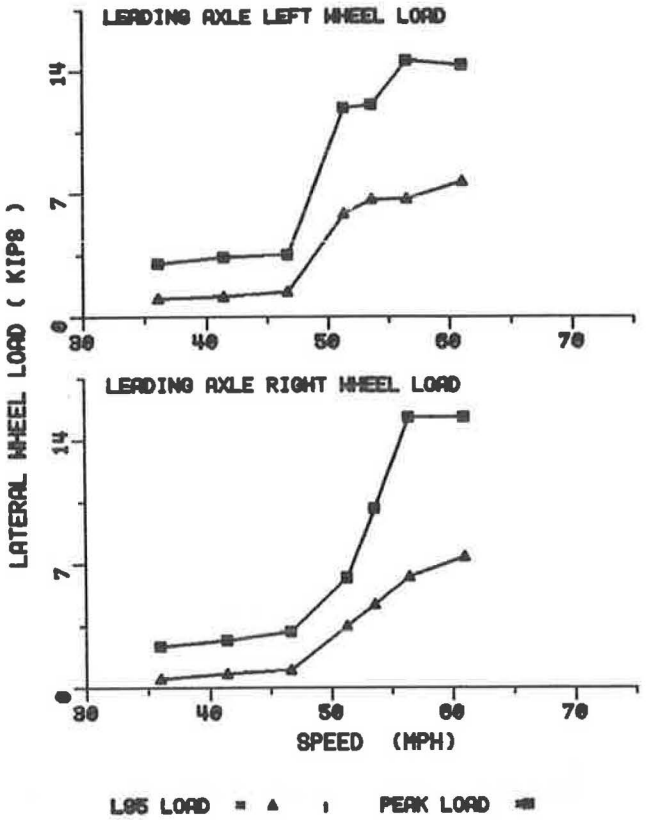

FIGURE 23 Peak lateral wheel load versus speed for a 100-ton empty, covered hopper car, measured during hunting using instrumented wheel set data.

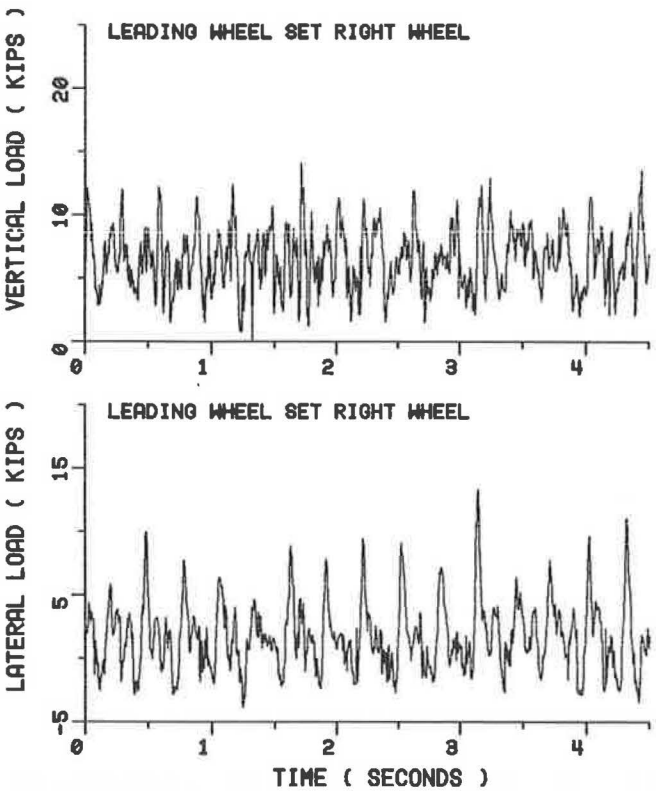

FIGURE 24 Wheel load time histories for a 100-ton empty, covered hopper car, measured at 61 mph during hunting using instrumented wheel set data.

The dynamic load environment produced by 125-ton cars during hunting is not reported in this paper because these data are not currently available.

CURVING

Negotiating curves with low wheel/rail forces is important from both the economic and safety points of view. The economic importance of curving ability can be viewed from the perspective of energy consumption and track maintenance. During curve negotiation, curve resistance, which is the power dissipated at the wheel/rail contact patch, must be overcome by added tractive effort that requires increased energy consumption. Excessive wheel/rail loads cause accelerated wheel/rail wear, truck component deterioration, and track damage. The ramification of all this is increased maintenance of vehicles and track structures, increased potential for derailment, and higher operating costs.

The forces developed between the wheel and rail depend on wheel/rail geometry (e.g., wheel profiles, degree of curvature, superelevation, etc.) and, most importantly, on the truck's primary suspension characteristics.

In sharp curves, depending on the speed of the vehicle, the outer wheel of the lead axle may assume flange contact with the high rail. This situation contributes to the wear of the wheel flanges as well as the gage face of the high rail. High lateral-to-vertical load ratios can cause the wheels to climb the rail or overturn the rail. The peak transient forces resulting

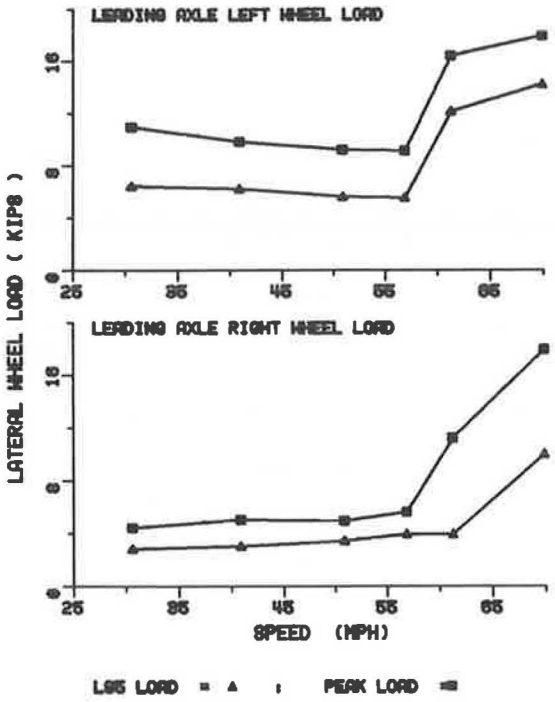

FIGURE 25 Peak lateral wheel load versus speed for a 100-ton loaded, covered hopper car, measured during hunting using instrumental wheel set data.

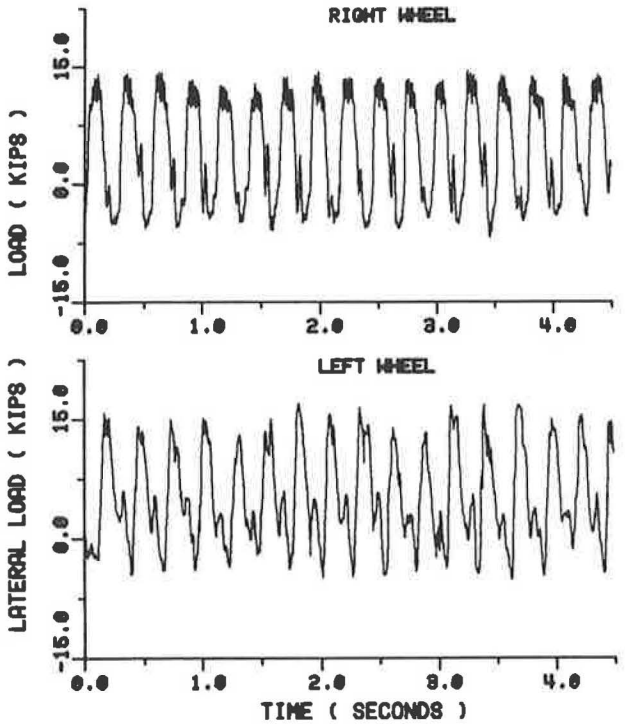

FIGURE 26 Lateral wheel load time histories for a 100-ton loaded, covered hopper car measured at 71 mph during hunting.

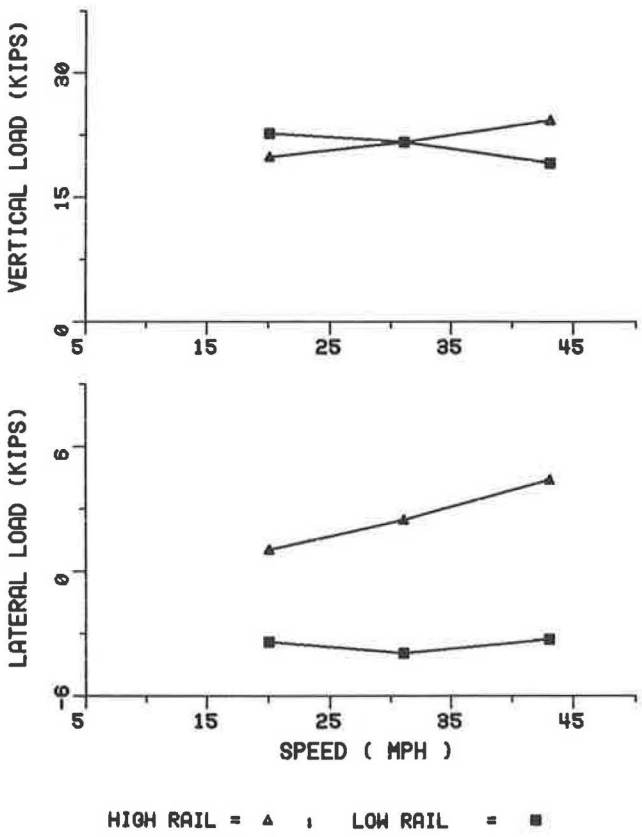

FIGURE 27 Average vertical and lateral load versus speed for a 70-ton loaded frame-braced truck, measured using instrumented wheel set data.

from hard flange impacts during curve entry and exit conditions can be larger than the steady-state forces. Some vehicles experience difficulties in entering and exiting sharper curves of relatively short spiral lengths. A loss of superelevation in such a spiral could create excessive body twist, and, if the torsional stiffness of the vehicle is high, wheel lifts and possible derailments could occur. Therefore, it is of utmost importance to determine the levels of the lateral wheel/rail loads, as well as the vertical load distribution on all four wheels of a truck.

70-Ton Cars

The Railmaster intermodal concept with 70-ton trucks was tested for curving performance at TTC (*12*). The steady-state curving performance characteristics were determined by evaluating the wheel/rail lateral and vertical forces, wheel set angles-of-attack, and L/V ratios at balance and underbalance speeds on curves ranging from 3 to 7.5 degrees.

The lateral and vertical wheel loads on the leading axle of the shared truck located at the leading end of the trailing van were measured using instrumented wheel sets. The curving tests were conducted on the FAST loop and the Balloon loop, providing track curvatures from 3.0 to 7.5 degrees. All curving tests were made with loaded cars in dry rail conditions at balance, overbalance, and below-balance speeds. The 3.0-, 4.0-, 5.0-, and 7.5-degree curved tracks had 2-, 3-, 4-, and 4.5-in. superelevations corresponding to 30.9-, 31.6-, 34.0-, and 29.3-mph balance speeds, respectively.

Figure 27 presents the results of mean lateral and vertical loads on the 5-degree curve. Note that the negative sign in this figure indicates that a low-rail lateral load is directed toward the flange. As seen in the figure, the lateral loads on the high rail increase with increasing speeds, as loads are shifted to the high rail. It should be noted that the individual lateral forces exerted on the rail act to spread the rails apart. Intersection of the vertical loads near 34 mph indicate that the theoretical balance speed was attained. The static wheel load on this lightly loaded truck was about 19 kips.

The mean values of the lateral loads, computed near balance speed as a function of track curvature, are shown in Figure 28. Note that the mean high-rail lateral loads increased from 1.7 kips on the 3-degree curve to 2.9 kips on the 7.5-degree curve. The corresponding low-rail lateral loads were 2.7 kips on the 3-degree curve and 5.2 kips on the 7.5-degree curve. The maximum high- and low-rail L/V ratios were 0.16 and 0.27 on the 7.5-degree curve, respectively.

The load environment seen under conventional 70-ton vehicles is not reported here because of a lack of curving data for this type of cars. The curving performance of this intermodal vehicle equipped with frame-braced trucks, high conicity wheels, and resilient primary suspension pads is believed to be superior to conventional vehicles with standard three-piece trucks.

100-Ton Cars

The High Performance, High Cube, Covered Hopper Car Project included a series of comprehensive tests to charac-

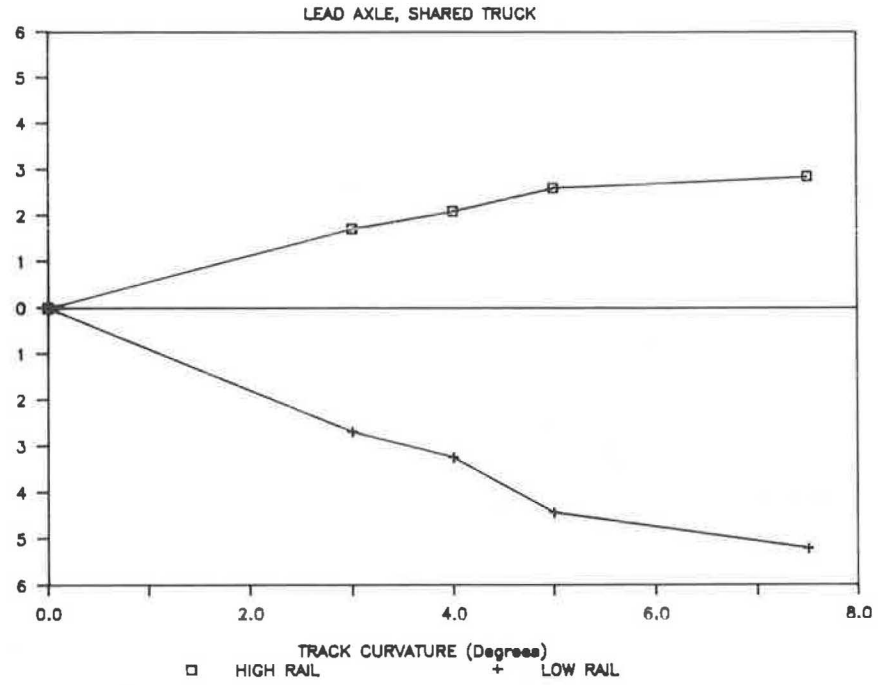

FIGURE 28 Average lateral load versus track curvature for a 70-ton loaded cross-braced truck, measured using instrumented wheel set data.

terize the curving performance of the baseline 100-ton covered hopper car described previously (*19*). The primary objective of the curving tests was to determine the vertical and lateral loads and the angles-of-attack developed during curve negotiation of the vehicle under various operating and track conditions.

The curving tests were conducted on various test tracks at the TTC, providing track curvatures ranging from 50 min. to 5 degrees. Instrumented wheel sets were used on the leading axle of the leading truck. The test runs were made at balance speed for each curve, as well as two speeds above and two speeds below the balance speed.

Figure 29 presents the results of mean lateral and vertical loads on the 5-degree curve versus test speed. The signs of the low-rail lateral wheel loads were changed to avoid overlapping of the curves; the negative sign indicates that a low-rail lateral load is directed toward the wheel flange. On the 5-degree curve, at severe unbalance speed of 10 mph, the mean lateral loads were as high as 14,000 lb on the low rail. At an above-balance speed of 45 mph, the mean values of the high-rail lateral loads increased to 13,000 lb. The individual wheel reaction forces were found to act to spread the rails apart, possibly resulting in gage widening on the track.

The vertical wheel loads showed similar trends in which the low-rail vertical loads decreased and the high-rail loads increased with increasing speeds for most of the curves. For the 5-degree curve, the mean values of the vertical wheel loads ranged from 25,000 to 43,000 lb, depending on the unbalanced superelevation. The intersection of the measured vertical wheel loads near 35 mph indicates that the theoretical balance speed on a 5-degree curve with 4 in. of superelevation was attained.

Figure 30 shows the mean lateral loads computed near balance speed, as a function of track curvature. As expected, the lateral loads increase with increasing curvature.

The lateral wheel loads produced on most curved tracks were in general compliance with fundamental curving behavior: they (a) tended to increase with increasing track curvatures and (b) shifted to the high-rail wheels with increasing speeds. On sharp curves below balance speed, the low-rail wheel of the lead axle experienced lateral loads up to 50 percent higher than the high-rail wheel. The net lateral load resulting from individual wheel loads on the track points toward the inside of the curve at these low speeds. Similarly, at above-balance speed, the high-rail wheel of the lead axle experiences higher lateral wheel loads than the low-rail wheel, partly because of flanging with the gage face of the high rail. The net lateral load exerted on the tracks by the lead wheel set points away from the center of the curve.

To evaluate the maximum levels of the lateral loads, which could cause permanent track deformation, the net axle loads with duration distance of 6 ft were investigated at severe unbalance conditions. It was found that the maximum net lateral lead axle load produced on the 5-degree curve at 45 mph (corresponding to 3 in. of deficiency in superelevation) was as high as 15,700 lb, pointing toward the outside of the curve. At 10 mph, corresponding to 3.6 in. of excess superelevation, the maximum net lead axle lateral load was on the order of 13,200 lb, pointing toward the inside of the curve.

125-Ton Cars

A test program undertaken to gather data to further the understanding of the 125-ton axle load environment and to develop a comparison between the 125- and 100-ton cars was conducted. The curving tests were conducted in the 5-degree curve and on tangent sections of the FAST loop. A total of three cribs was instrumented in the curved section for load

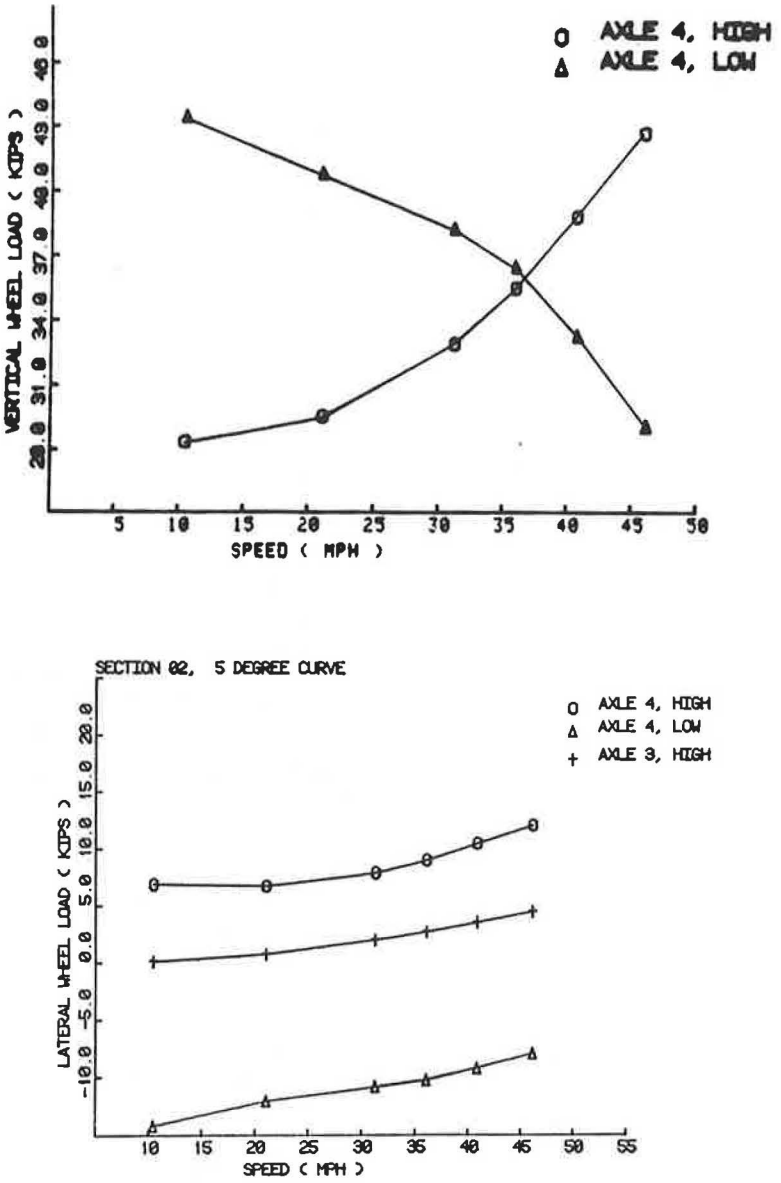

FIGURE 29 Wheel loads versus speed for a 100-ton loaded, covered hopper car, measured on a 5-degree curve using instrumented wheel set data.

and deflection measurements. The tests were run at speeds of 10, 20, 25, 30, 35, and 40 mph on tangent and curved tracks. A total of 25 laps was also run at 40 mph in order to get statistical distribution of the wheel loads.

Figure 31 shows the maximums of vertical and lateral wheel loads (averaged over three instrumented cribs) of leading trucks of all five 125-ton cars on the 5-degree curved and tangent track as a function of test speed. The peak vertical loads on tangent track remain slightly above the static load level of 39 kips at speeds from 10 to 40 mph. The maximum vertical loads show a general trend in which the high-rail loads increase and low-rail loads decrease with speed because of excess superelevation. However, intersection of the vertical load curves does not occur at the theoretical balance speed of 34 mph, because the loads shown in Figure 31 represent maximum vertical loads rather than average vertical loads.

The low-rail lateral loads in Figure 31 appear to be higher than the high-rail loads at all speeds except 40 mph. In general, the low-rail steady-state lateral loads should follow the same trend and decrease with speed like the low-rail vertical loads, but they increase along with the high-rail loads at speeds above 30 mph. The reason is that the lateral loads shown in Figure 31 are the dynamic lateral rail loads that occur over approximately 10 ft of curved track segment. Consequently, the lateral rail loads include steady-state as well as dynamic loads and do not follow the trend displayed by the vertical rail loads.

The statistical analysis results are shown in plots of probability distribution functions in Figure 32, for peak vertical loads. For the 125-ton cars, the median vertical loads on the high rail were about 46,000 lb, and they were 36,000 lb on the low rail at 40 mph.

Comparison of the load distribution curves indicates that the 125-ton car vertical load frequency of exceedance levels

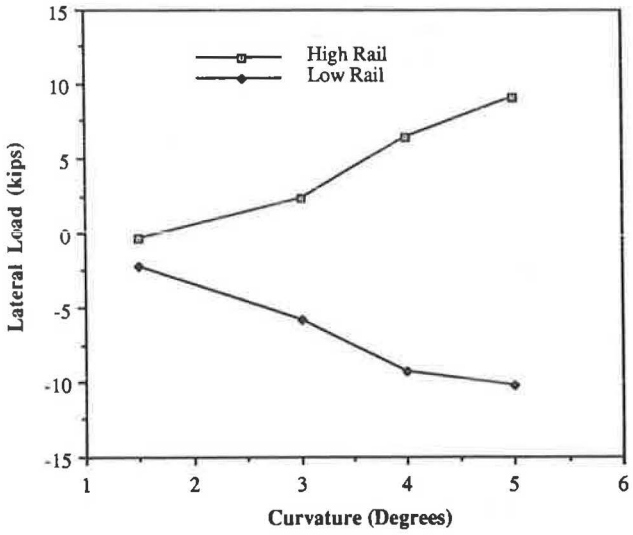

FIGURE 30 Mean lateral wheel load versus track curvature for a 100-ton loaded, covered hopper car, measured using instrumented wheel set data.

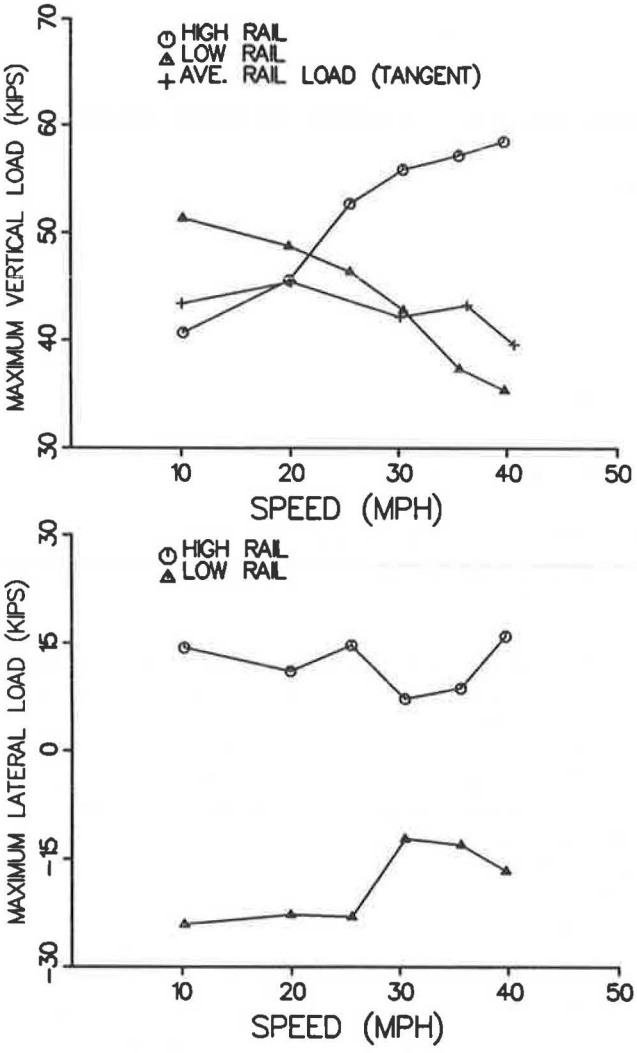

FIGURE 31 Maximum vertical and lateral rail loads versus speed for a 125-ton covered hopper car, measured using wayside data.

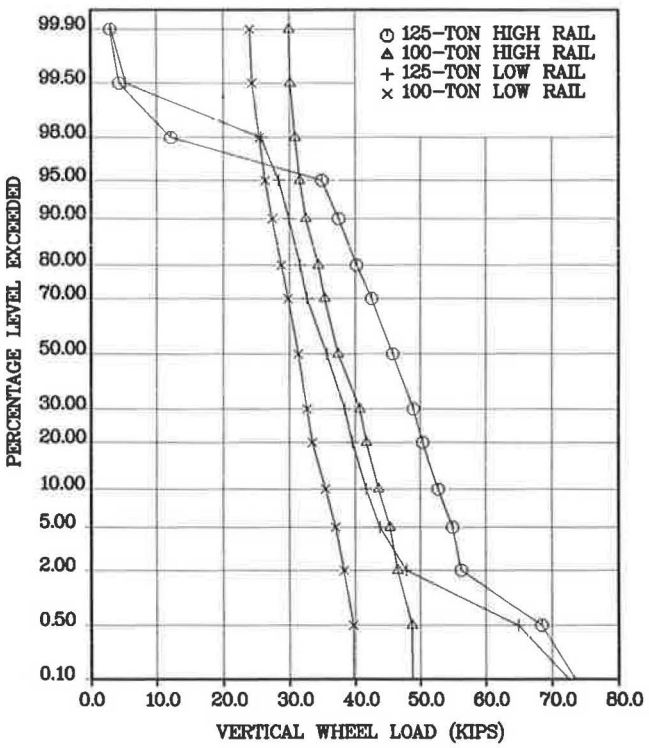

FIGURE 32 Probability distribution of peak vertical rail loads for 100- and 125-ton cars, measured at 40 mph.

from 2 to 98 percent was 20 percent higher than that of the 100-ton cars. The maximum vertical loads with a frequency of less than one per 100 axles were up to 45 percent higher for the 125-ton cars than for the 100-ton cars. The importance of this information is that higher dynamic loads developed under 125-ton cars would be significantly more damaging to the track structure than those under 100-ton cars.

CONCLUSIONS

Based on the results presented herein, the following observations and conclusions were made:

- The high-speed track testing of standard 70-, 100-, and 125-ton freight cars indicated that these cars experience bolster loads in excess of 1.8 times the static load as a result of a variety of track irregularities. The most damaging sites with multiple periodic vertical track irregularities excite the vehicles harmonically. The loads produced by the harmonically excited vehicles appear to be causing further loss of track geometry from the initial irregularity. At these sites the extent of damage appears to be growing with traffic.
- Because of a lack of effective damping during bounce resonance of a standard freight car, successive cycles of suspension spring bottoming produce extremely high vertical loads. The controlled test results indicate that when excited by periodic, parallel, 39-ft low-rail joints with 0.75-in. maximum surface profile deviations, peak dynamic vertical wheel loads for 70-, 100-, and 125-ton cars can be as high as 3 to 5 times the static wheel load. The revenue track test results agree with the controlled test results in that the vertical wheel loads in

excess of three times the static load occur as a result of a series of parallel rail joints occurring on open track with continuously welded rail.

- The maximum dynamic vertical loads resulting from roll resonance ranged from 1.8 to 3 times the static wheel load for loaded 70-, 100-, and 125-ton cars. All car types exhibited extensive wheel unloading.
- As a result of excessive car body roll, suspension bottoming occurs, and the resulting violent undamped body motions cause excessive loading of one side of the track with the other side lifting clear of the track structure. Asymmetric loading of the track structure along the direction of travel results in accelerated deterioration and additional loss of track geometry. With increasing cross-level elevation, the vehicles operating over the same track section would experience higher and higher loads bringing about additional geometry loss resulting in increased derailment propensity.
- At and above the critical hunting speed of a vehicle, very large dynamic lateral loads are exerted on the vehicle and track at frequencies from 2 to 4 H. The peak cyclic lateral loads measured on a 100-ton empty and loaded covered car were as high as 15 to 20 kips, respectively. These loads can cause wide gage and lateral alignment problems on tangent track. Truck hunting, when combined with track irregularities, can create a potential for wheel climb derailment.
- Because the energy necessary to sustain hunting motions is eventually provided by the forward motion of the vehicle, the excessive lateral and yaw motions of the wheel set increase the rolling resistance, resulting in increased energy consumption.
- During curve negotiation of a railway vehicle, the lateral and vertical loads shift to high rail with increasing speeds as a result of overbalance superelevation. The individual lateral loads exerted on the rail act to spread the rails apart.
- A standard North American freight car equipped with conventional three-piece trucks with no primary suspension system achieves its guidance on sharper curves by the wheel flanges. The resulting high wheel/rail forces lead to problems associated with increased wear, truck deterioration, and track damage.
- The increased energy consumption during curving results from the energy dissipated at the contact patch, which must be overcome by added tractive effort.
- Preliminary results obtained from a series of recent track testing of 100- and 125-ton cars indicate that the average 125-ton car vertical wheel loads were 20 percent higher than those of the 100-ton cars on a 5-degree curve. The peak wheel/rail impact loads during curving were 45 percent higher for the 125-ton cars than for the 100-ton cars. Higher dynamic loads developed under 125-ton cars would be more damaging to the track structure. The ongoing 150 million gross tons of operation of heavy axle load cars on the FAST loop will verify and translate this load environment into track deterioration.
- The results of dynamic load testing suggest that vehicle suspension characteristics of heavier cars will have a major effect on the performance and life of the track structure.
- For conventional North American freight cars, the low-frequency dynamic wheel/rail loads associated with suspension dynamics are transmitted to and damaging for the vehicle/track structure. The analysis of the effects of loads in excess of the design values on fatigue life indicates that these high-magnitude, low-frequency loads cause considerable component fatigue damage.
- Inadequate suspension damping adversely influences the dynamic loads imposed on track with imperfect surface characteristics. Even with "questionable" track conditions, railway vehicles equipped with premium suspension systems do not produce excessive dynamic loads. However, standard suspension systems do produce dynamic loads beyond the design limits of vehicle/track components.
- An economic study focusing on the relative cost of maintenance of track and truck components as affected by excessive dynamic loads should be conducted.

REFERENCES

1. E. H. Law and N. K. Cooperrider. A survey of Railway Vehicle Dynamics Research. *Journal of Dynamics Systems, Measurement, and Control*, ASME, Vol. 96, No. 2, June 1974.
2. F. B. Blader. Development and Applications of a General Rail Vehicle Dynamic Computer Model (NUCARS). Presented at the ASME Winter Annual Meeting, Nov. 1988.
3. *Proc., International Conference on Wheel/Rail Load and Displacement Measurement Techniques.* Report DOT-TSC-UMTA-82-3. UMTA, U.S. Department of Transportation, Jan. 19, 1981.
4. S. Kalaycioglu and S. K. Punwani. *High Performance/High Cube Covered Hopper Program, Base Car Dynamic Performance Tests, Volume 4—Summary.* Report R-581. Association of American Railroads, Chicago, Ill., June 1984.
5. P. V. RamaChandran and M. M. ElMadany. *Truck Design Optimization Project Phase-II.* FRA/ORD-81/48; Final Report. FRA, Sept. 1981.
6. N. K. Cooperrider, E. H. Law, and R. H. Fries. *Freight Car Dynamics, Field Test Results and Comparison with Theory.* Report FRA/ORD-81/46. FRA, June 1981.
7. R. H. Prause, H. D. Harrison, J. C. Kennedy, and R. C. Arnlund. *An Analytical and Experimental Evaluation of Concrete Cross Tie and Fastener Loads.* Report FRA/ORD-77/71. FRA, Dec. 1977.
8. V. Sharma, W. H. Sneed, and S. K. Punwani. Freight Equipment Environmental Sampling Test—Description and Results. *Proc., ASME Rail Transportation Spring Conference*, Chicago, Ill., April 1984.
9. R. A. Poclington. The B. R. Load Measuring Wheel. *Proc., International Conference on Wheel/Rail Load and Displacement Measurement Techniques.* Report DOT-TSC-UMTA-82-3. U.S. Department of Transportation, Jan. 1981.
10. H. D. Harrison and D. R. Ahlbeck. Development and Evaluation of Wayside Wheel/Rail Measurement Techniques. *Proc., International Conference on Wheel/Rail Load and Displacement Measurement Techniques.* Report DOT-TSC-UMTA-82-3. U.S. Department of Transportation, Jan. 1981.
11. S. K. Punwani. Measurement of Wheel/Rail Forces on the High Cube, High Performance Covered Hopper Car Project. *Proc., ASME Rail Transportation Spring Conference.* Chicago, Ill., April 1984.
12. G. B. Anderson, S. Kalaycioglu, and S. P. Singh. *High Productivity Integral Train Program, Railmaster System Concept Tests, Volume 1, Summary.* Report R-653. Association of American Railroads, Chicago, Ill., Aug. 1987.
13. S. Kalaycioglu and S. K. Punwani. *High Performance/High Cube Covered Hopper Program, Base Car Dynamic Performance Tests. Volume 1—Rock-and-Roll and Bounce.* Report R-566. Association of American Railroads, Chicago, Ill., April 1984.
14. P. Singh Satya, J. T. Dincher, and S. K. Punwani. *High Performance/High Cube Covered Hopper Program, High Cube 2000 Prototype Dynamic Performance Tests, Summary.* Report R-636. Association of American Railroads, Chicago, Ill., Aug. 1987.
15. S. Kalaycioglu and A. Tajaddini. *Locating Vertical Track Irregularities Which Cause Excessive Vehicle Loads.* Report R-694. Association of American Railroads, Chicago, Ill., March 1988.
16. S. Kalaycioglu and A. Tajaddini. Investigation of Vertical Track Irregularities: Phase 2, Vehicle Track System Testing. Presented at the ASME Winter Annual Meeting, Nov. 1988.

17. S. Kalaycioglu and S. K. Punwani. *Lateral Stability of a 100-Ton Covered Hopper Car Equipped with Conventional Trucks*. Presented at the ASME Winter Annual Meeting, Nov. 1985.
18. D. R. Ahlbeck, H. D. Harrison, and S. L. Noble. *An Investigation of Factors Contributing to Wide Gage on Tangent Track*. Presented at the ASME Winter Annual Meeting, Nov. 1975.
19. S. Kalaycioglu, A. V. Arslan, and S. K. Punwani. *High Performance/High Cube Covered Hopper Program, Base Car Dynamic Performance Tests, Volume 3—Curving*. Report R-572. Association of American Railroads, Chicago, Ill., April 1984.

Publication of this paper sponsored by Committee on Railroad Track Structure System Design.